Journal of Neuroscience Methods 291 (2017) 221–226

Contents lists available at ScienceDirect

Journal of Neuroscience Methods

journal homepage: www.elsevier.com/locate/jneumeth

Automated touch sensing in the mouse tapered beam test using Raspberry Pi

Dirk Jan Ardesch[a,b], Matilde Balbi[a,c], Timothy H. Murphy[a,c,*]

[a] Department of Psychiatry, Kinsmen Laboratory of Neurological Research, University of British Columbia, Vancouver, British Columbia V6T 1Z3, Canada
[b] Master Program Neuroscience and Cognition, Graduate School of Life Sciences, Utrecht University, The Netherlands
[c] Djavad Mowafaghian Centre for Brain Health, University of British Columbia, Vancouver, British Columbia, V6T 1Z3, Canada

HIGHLIGHTS

- Easy-to-implement adaptation to existing tapered beam test in mice.
- Automation of foot fault detection saves time and increases objectivity.
- Inexpensive hardware and open-source software in Python.

GRAPHICAL ABSTRACT

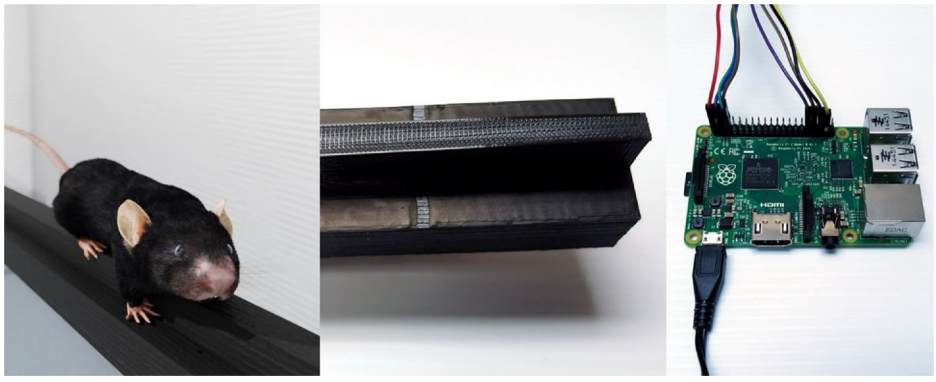

ARTICLE INFO

Article history:
Received 13 June 2017
Received in revised form 23 August 2017
Accepted 24 August 2017
Available online 30 August 2017

Keywords:
Tapered beam test
Raspberry Pi
Automation
Mouse
Behavior
Stroke

ABSTRACT

Background: Rodent models of neurological disease such as stroke are often characterized by motor deficits. One of the tests that are used to assess these motor deficits is the tapered beam test, which provides a sensitive measure of bilateral motor function based on foot faults (slips) made by a rodent traversing a gradually narrowing beam. However, manual frame-by-frame scoring of video recordings is necessary to obtain test results, which is time-consuming and prone to human rater bias.
New method: We present a cost-effective method for automated touch sensing in the tapered beam test. Capacitive touch sensors detect foot faults onto the beam through a layer of conductive paint, and results are processed and stored on a Raspberry Pi computer.
Results: Automated touch sensing using this method achieved high sensitivity (96.2%) as compared to 'gold standard' manual video scoring. Furthermore, it provided a reliable measure of lateralized motor deficits in mice with unilateral photothrombotic stroke: results indicated an increased number of contralesional foot faults for up to 6 days after ischemia.
Comparison with existing method: The automated adaptation of the tapered beam test produces results immediately after each trial, without the need for labor-intensive post-hoc video scoring. It also increases objectivity of the data as it requires less experimenter involvement during analysis.

* Corresponding author at: 2255 Wesbrook Mall, Detwiller Pavilion, Vancouver, B.C. V6T 1Z3, Canada.
E-mail address: thmurphy@mail.ubc.ca (T.H. Murphy).

http://dx.doi.org/10.1016/j.jneumeth.2017.08.030
0165-0270/© 2017 Elsevier B.V. All rights reserved.

Conclusions: Automated touch sensing may provide a useful adaptation to the existing tapered beam test in mice, while the simplicity of the hardware lends itself to potential further adaptations to related behavioral tests.

© 2017 Elsevier B.V. All rights reserved.

1. Introduction

Motor deficits are a common phenotype in rodent models of neurological disease such as stroke or traumatic brain injury (Caleo, 2015; Yang et al., 2013). Tests of motor function can serve as important readouts of underlying neurological function and are often used to assess the severity of a neurological condition or the efficacy of a new treatment (Brooks and Dunnett, 2009). One of the tests frequently used in mice is the tapered beam test (Bye et al., 2007; Schallert et al., 2002). This test requires the animal to traverse an elevated beam that becomes gradually narrower towards the end (Fig. 1). Side ledges extend to the left and right side underneath the beam, such that a mouse that slips will put its foot onto the side ledge to retain balance. The number of foot faults (slips) made by the mouse provides an inndication of motor function and is asymmetrical in case of unilateral deficits (Schallert et al., 2002).

Although the tapered beam test can provide sensitive measurements of (lateralized) motor deficits, it requires laborious frame-by-frame scoring of video recordings and is therefore prone to systematic bias introduced by the human rater. Thus, automation of behavioral tests like the tapered beam test can help maximize objective measurement and reduce time spent on data processing.

We present an easy-to-use automated adaptation of the tapered beam test in mice. Using low-cost capacitive touch sensors connected to a Raspberry Pi single-board computer, foot faults onto the side ledge are detected in real-time and results are available immediately after each trial. The goal of this study was to assess the sensitivity of automated foot fault detection and to confirm the validity of the automated tapered beam test as a measure of lateralized motor deficits. We hypothesized that this test 1) achieves high sensitivity for foot fault detection as confirmed by 'gold standard' video analysis, and 2) provides a valid measure of lateralized motor deficits after unilateral stroke.

2. Methods and materials

2.1. Components and construction

All components necessary for automated foot fault detection in the tapered beam test are listed in Table 1. For a step-by-step construction tutorial see Supplementary video.

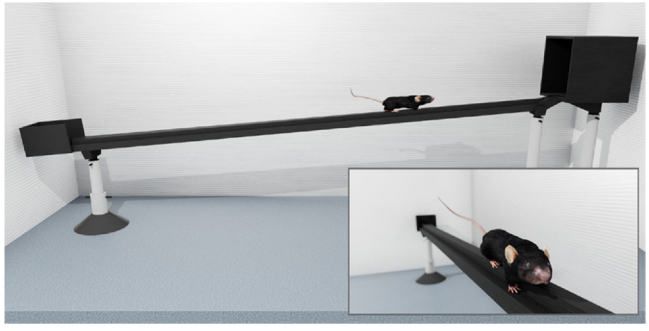

Fig. 1. Rendered image of the tapered beam. The apparatus includes a loading area at the left end and a refuge box at the right end of the beam. Inset: close-up view of a mouse stepping onto the side ledge (foot fault).

The tapered beam was constructed from five individually 3D-printed modules (Supplementary File 1) and followed the dimensions typically used in the mouse literature (e.g. Bye et al., 2007; Corrigan et al., 2012). Thus, the beam measured 100 cm in length, tapering from 3.5 cm to 0.5 cm from one end to the other, and featured a wider base part 1 cm below the upper surface of the beam to provide side ledges extending 1 cm to the left and right (Fig. 1 inset). Although the 3D-printable design was optimized for easy implementation of automated foot fault detection, any regular tapered beam could in principle be used as well.

Touches onto the side ledges were recorded through a layer of conductive paint (Bare Conductive, London, UK) which was divided into 23 non-interconnected surfaces per side measuring 4×1 cm each, together spanning around 92 cm of the beam's total length (Fig. 2A). These conductive paint surfaces served as input electrodes for four 12-channel capacitive touch sensors (Adafruit Industries, New York, NY, USA) which together provided 48 channels. The remaining two input electrodes were painted on the top surface at either end of the beam to record the start and finish times of each trial. As the water-based paint dissolves easily when cleaning the beam with soap and water or alcohol, we applied a layer of polyurethane finish to protect the electrodes. This procedure, despite insulating the paint, did not hinder the recording of touches since capacitive touch sensors do not require direct electrical contact. The electrodes were connected to the touch sensors by means of jumper wires, which were plugged into the beam to make contact with the conductive paint on one end, and connected to header pins on the touch sensor on the other end (Fig. 2B).

The capacitive touch sensors were connected to a Raspberry Pi single-board computer (Fig. 2C) to process and store the data using custom software written in Python (van Rossum, 1995). These scripts are provided in Supplementary File 2. Readout parameters include the total number of foot faults, number of foot faults per side, time to traverse the beam, time to first foot fault, and (approximate) distance to first foot fault. More information such as the exact

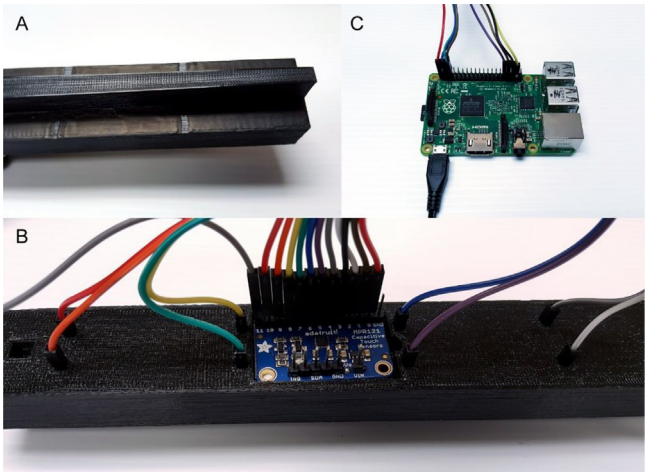

Fig. 2. Assembly of the automated tapered beam apparatus. A) Electrode surfaces are painted onto the side ledges to the left and right of the beam (top view). B) Jumper wires connect the electrodes to the capacitance sensor chips (bottom view). C) Logic and power connections are fed into the Raspberry Pi computer.

Table 1
Parts list for automated foot fault detection in the tapered beam test.

Component	Quantity	Supplier	Part number
Raspberry Pi	1	Newark	38Y6467
12-channel capacitive touch sensor breakout – MPR121	4	Adafruit Industries	1982
Bare Conductive electric paint	50 mL	Bare Conductive/Adafruit Industries	1305
Jumper wires M/F 150 mm	60	Sparkfun	PRT-12794
Wood Shield Clear Coat polyurethane finish spray	1	Home Hardware a.o.	1877-017
Optional: Pi Camera version 2	1	Newark	77Y6521

time, duration, or distance of every individual foot fault is also readily available. All results are stored in a comma-separated file format for convenient transfer to any major statistical software package for further analysis. In addition, a Pi Camera can be connected to the Raspberry Pi to automatically co-record video with each trial if so desired.

2.2. Validation

2.2.1. Study design

The study consisted of two separate experiments. In Experiment 1, we evaluated the sensitivity of the automated tapered beam test by comparing the capacitive touch sensor data against 'gold standard' results obtained by video analysis in a sample of healthy mice. In Experiment 2, we assessed its construct validity by means of an additional sample of mice tested before unilateral stroke until one week after stroke.

2.2.2. Animals

All animal procedures were approved by the University of British Columbia Animal Care Committee and conformed to the Canadian Council on Animal Care and Use guidelines. A total of 25 naïve C57Bl/6 mice (The Jackson Laboratory) were used in this study. Animals were housed with up to 4 cage mates in a 12 h light-dark cycle at 21–24 °C with *ad libitum* access to water and food.

Nine out of the 25 mice participated in Experiment 1 and were sourced from surplus animals for a calcium imaging study using the genetically encoded calcium indicator GCaMP6s. These transgenic GCaMP6s-negative mice (all male, 4–5 months of age) were produced by crossing Emx1-cre (B6.129S2-Emx1$^{tm1(cre)Krj}$/J, Jax no. 005628), CaMK2-tTA (B6.Cg-Tg (Camk2a-tTA) 1Mmay/DboJ, Jax no. 007004), and TITL-GCaMP6 s (Ai94; B6.Cg-Igs7$^{tm94.1(tetO-GCaMP6s)Hze}$/J, Jax no. 024104) strains (Madisen et al., 2012). PCR confirmed the absence of at least the TITL-GCaMP6 s or CaMK2-tTa sequence, resulting in the absence of GCaMP6 s expression.

The remaining 16 mice (7 female, 5–6 month of age) participated in Experiment 2 and were included from an ongoing stroke study. These mice (B6.Cg-Tg(Slc32a1-COP4*H134R/EYFP)8Gfng/J, Jax no. 014548) expressed VGAT channelrhodopsin2 for optogenetic stimulation and had undergone surgical implantation chronic transcranial windows around one week before the start of the experiment as previously described (Silasi et al., 2016).

2.2.3. Photothrombotic stroke

Mice participating in Experiment 2 were head-fixed after which a photosensitive dye solution Rose Bengal (R3877-5G, SIGMA-ALDRICH, USA) was injected intraperitoneally (0.01 mL/g body weight). Two minutes after injection, a 40 mW diode pump solid state 532 nm laser MGM-20 (Beta Electronics, Columbus, OH, USA) was positioned over the left sensorimotor cortex for 13 min to produce a unilateral photothrombotic stroke in awake head-fixed mice (Balbi et al., 2017).

2.2.4. Procedure

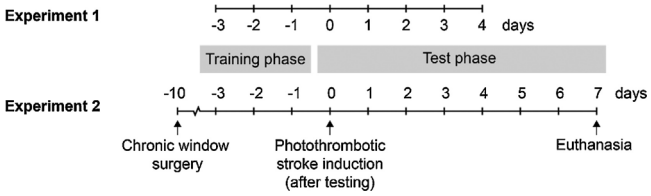

Fig. 3. Experimental procedure. Experiment 2 consisted of three more test days than Experiment 1 to allow for follow-up of motor deficits until a week after stroke.

2.2.4.1. Experiment 1. Mice were accustomed to the task in two ($N = 5$) or three ($N = 4$) training days of three trials each day. A small dark box containing some nesting material from the home cage was placed at the narrow end of the beam to motivate animals to traverse the beam. During each training trial, mice were positioned at the wide end of the beam and were allowed to freely explore the apparatus for 3 min before being gently nudged by the experimenter towards the narrow end. On the first day, mice were given 60 s of time in the dark box to facilitate the association of traversing the beam with 'safety'. Since most mice readily traversed the beam after the first training day, this time was decreased to 30 s on subsequent training and test days. After training, mice were tested during 5 consecutive days with 3 trials per day (Fig. 3). Data from the touch sensors as well as video recordings were collected for these test trials.

2.2.4.2. Experiment 2. All conditions for the training phase were identical to Experiment 1 except that all mice in this sample ($N = 16$) underwent three days of training. After training, mice were tested during 8 consecutive days with 3 trials per day (Fig. 3). Photothrombotic stroke was induced in the left sensorimotor cortex after the first test day (Day 0), immediately after which mice were randomly assigned to either one of three optogenetic stimulation protocols for one hour as part of the ongoing stroke study. As this stimulation paradigm was not the focus of the current study, we did not include this factor in our hypotheses. Mice were euthanized at the end of Day 7.

2.2.5. Analysis

2.2.5.1. Experiment 1. All foot faults (operationalized as positioning of the entire foot onto the side ledge, e.g. Fig. 1 inset) and their corresponding electrode locations were obtained from the video recordings by an observer blinded to the capacitive touch sensor results. Results from the video recordings and touch sensors were compared against each other by a second observer. Taking the video results as the gold standard, foot faults detected by the capacitive touch sensors were classified as true positives (a foot fault was recorded in both datasets), false positives (a touch was recorded by the touch sensors without a corresponding foot fault in the video results), and false negatives (a foot fault was recorded in the videos without a corresponding foot fault in the touch sensor results). True negatives were not defined in this case because the default situation was a 'no touch'. Steps onto the start and finish electrodes, which were not technically foot faults, were also included. From these data, the sensitivity and positive predictive value of touch-based

Table 2
Classification of the automated tapered beam test.

N touches (video analysis)	316
True positives	304
False positives (tail and nose touches)	28
False negatives	12
Positive predictive value	91.6%
Sensitivity	96.2%

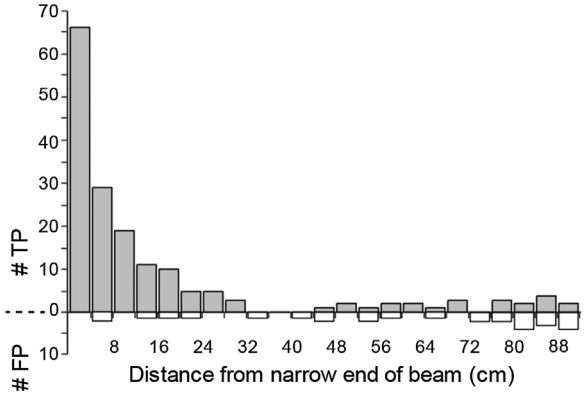

Fig. 4. Distribution of true positive foot faults (# TP) and false positive touches (# FP) along the main axis of the beam. Bars represent total number of touches recorded over 135 trials.

foot fault detection were calculated. In addition, false positives and false negatives were revisited in the video recordings to explore possible causes of disagreement.

2.2.5.2. Experiment 2. Number of foot faults on the left side ledge and right side ledge were obtained from the capacitive touch sensors and averaged over the three trials per day. Repeated measures ANOVAs were used to test effects of measurement day and optogenetic stimulation group on the number of foot faults. Analysis was performed in R and GraphPad Prism 7 (GraphPad Software, 2017; R Core Team, 2017). All p values <.05 were considered statistically significant.

3. Results

3.1. Experiment 1

All animals had learned the task by the end of the training sessions, i.e. they could traverse the beam in a swift manner while avoiding the side ledges. Video analysis revealed a total of 450 touches onto the electrodes (including the start and finish electrodes that were not located on the side ledges). Of these, 400 were detected by the touch sensors as well. In all cases, the location of the touch as determined by video analysis matched the location obtained from the touch sensors. Strikingly, 76% of false negatives arose from the start electrode only, which was found to be badly wired to the touch sensor chip. This defect has since been rectified in the new version of the device. As this particular electrode was used to detect the start of each trial rather than foot faults, we decided to exclude all 134 touches onto the start electrode from further analysis. The resulting summary statistics are depicted in Table 2.

Not surprisingly, the number of foot faults recorded at a given electrode location increased closer to the narrow end of the beam (Fig. 4). Moreover, false negatives seemed to be evenly spread over the electrodes (data not shown). False positives were exclusively due to touches by the tail or the nose, which were most common when the mouse was stationary on the beam (i.e., no touches were recorded when there was in fact no touch). Importantly, the duration of false positive touches was lower (M = 42.9 ms, SD = 46.6 ms) than the duration of true positive foot faults (M = 343.3 ms, SD = 205.4 ms), t(157.02) = 15.18, p < .001, two-tailed. This makes it possible for the software to detect potential false positives and prompt the user to review the event in question, or automatically exclude the result.

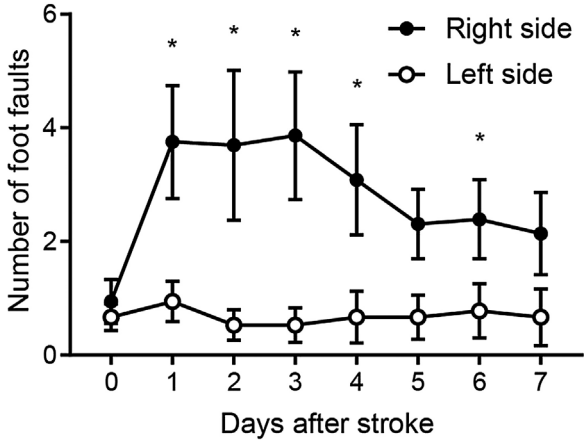

Fig. 5. Performance on the tapered beam before (Day 0) and after stroke (Days 1–7). Asterisks indicate significant differences (p < .05) in number of right-sided foot faults compared to Day 0. Error bars represent standard error of the mean (N = 12).

3.2. Experiment 2

Of the 16 animals, 13 had learned the task by the end of the training sessions. Three animals did not make any effort to avoid the side ledges (i.e., they did not achieve a symmetrical baseline score of a few foot faults per trial) and were therefore excluded from further analysis. One other animal was excluded due to technical problems with intraperitoneal injection of Rose Bengal (only a small amount of the required volume was successfully administered, resulting in the absence of a clear ischemic area as confirmed by laser speckle imaging). All subsequent analyses were performed on the remaining 12 animals.

A two-way repeated-measures ANOVA with optogenetic stimulation group (3 levels) and time (8 levels) as independent variables and number of foot faults on the right side as dependent variable revealed, as expected, a significant main effect of time, F(7, 63) = 7.32, p < .001; as well as a significant interaction between time and group, F(14, 63) = 2.14, p = .02. However, no main effect of group was found F(2, 9) = 0.294, p = .75. Since the optogenetic stimulation paradigm was not part of the main aim of this study, the data of the three groups was pooled to increase statistical power in the subsequent tests.

The pooled data is summarized in Fig. 5. A two-way repeated-measures ANOVA on the pooled data with side (left vs right) and time (8 levels) as independent variables and number of foot faults as dependent variable revealed significant main effects of side, F(1, 22) = 6.14, p = .02; and time, F(7, 154) = 3.72, p = .001; as well as a significant interaction between the two factors, F(7, 154) = 3.82, p < .001. Post-hoc tests showed that the number of contralesional foot faults (i.e., on the right side) was increased compared to the pre-stroke baseline on Day 1, 2, 3, 4, and 6 (all p < .05), with a trend on Day 5 (p = .058), corrected for multiple comparisons with Dunnett's test. Importantly, the number of ipsilesional foot faults (i.e., left side) did not change between the pre-stroke baseline and any of the subsequent days (all p > .05). These results confirm the observation that the tapered beam test is sensitive to unilateral motor

deficits and supports our hypothesis that this observation holds for the automated version of the test as well.

4. Discussion

We present an adaptation of the tapered beam test that allows for automated detection and processing of foot faults using capacitive touch sensors. The system is relatively easy to construct using low-cost materials and provides reliable detection of foot faults made by mice traversing the beam. The main advantage of this adapted task is that results are available immediately after each trial, which reduces labor-intensive post-hoc video analysis. In addition, the computerized processing of the data prevents any systematic bias caused by observer fatigue or inter-rater variability. In our validation sample of >100 trials the automated tapered beam test achieved high sensitivity when compared to 'gold standard' video analysis. Moreover, its validity as a test of motor function was confirmed in a second sample of mice tested before and after photothrombotic stroke. As expected, mice made more foot faults with the affected (contralesional) limbs for several days after stroke as compared to baseline, whereas the number of foot faults made with the unaffected (ipsilesional) limbs remained unchanged.

Although the system provides clear advantages over the standard tapered beam test, there are some limitations that need to be considered. First, the system does not distinguish between foot faults made by forelimbs, hindlimbs, or both limbs at the same time. Although some studies have assessed fore- and hindlimb foot faults separately (Lipsanen et al., 2011; Tarlac et al., 2013; Zhao et al., 2005), other studies have simply combined them into a total score per side (Bye et al., 2007; Ng et al., 2012; Semple et al., 2010; Spanevello et al., 2013). In our observations, most foot faults (81.5%, $N = 60$ trials) consisted of a forelimb touch immediately followed by a hindlimb touch, and resulted in a single response from the sensors. It appears therefore that the distinction between fore- or hindlimb foot faults is not of critical importance for the reliability of this test, which is further strengthened by our finding of significant differences between performance of mice before versus after stroke obtained through automated foot fault detection.

Second, the results can be contaminated by false positives caused by touches of the nose or tail when the animal has paused its crossing of the beam. Fortunately, these touches can generally be filtered out due to their shorter duration. Nevertheless, it may be advisable to co-record video if the user wants to be completely sure no foot fault is accidentally excluded. In this case, the software will automatically acquire video using the Pi Camera and keep track of the exact time and electrode location at which potential false positive results are recorded for later manual confirmation by the user.

Third, the touch sensors did not successfully detect all foot faults (3.8% missed). Although gold standard video analysis may not reach perfect sensitivity either and the incidence of false negatives was generally low, fine-tuning of the electronics hardware and software may help to achieve even higher sensitivity. For example, the sensitivity of the capacitance sensors is adjustable and may be further optimized.

This study hopes to contribute to the continuing effort of automating research methods in rodents (Schaefer and Claridge-Chang, 2012). For example, similar Raspberry Pi-based methods have recently been used to automate weighing and head-fixed GCaMP imaging protocols in a home cage environment (Bolaños et al., 2017; Murphy et al., 2016). In this light, a possible next goal may be to make the tapered beam test accessible from the home cage to further reduce stress experienced by the animals due to handling and changing environments (Sorge et al., 2014). RFID identification of individual animals could be used to determine which mouse is entering the apparatus and block entry to the apparatus after a certain number of trials (Bolaños et al., 2017; Weissbrod et al., 2013). An additional food reward could be presented at the end of the beam to motivate mice to initiate trials. The adapted test could be useful as a time-efficient alternative alongside other motor tests in mice such as the popular but laborious single-pellet reaching test, of which an automated version currently only exists for rats (Chen et al., 2014; Farr and Whishaw, 2002; Fenrich et al., 2015).

Since the technology behind the automated tapered beam test is simple and easy to implement, it could arguably be adapted for use in other behavioral tests that make use of touches or steps of the animal such as the cylinder test, ladder rung test, or ledged grid walking test (Metz and Whishaw, 2009; Schallert and Tillerson, 2000; Tennant and Jones, 2009). Similarly, it may be used to power do-it-yourself versions of already available (but expensive) cognitive tests, such as the 5-choice serial reaction time task (Mar et al., 2013). The open source software additionally ensures complete flexibility of the experimental design as well as data processing and output.

In conclusion, capacitive touch-based detection of foot faults in the tapered beam test for mice provides a cost-effective and easily implementable alternative to conventional video analysis. The method has high sensitivity and appears to reliably probe motor performance mice before and after photothrombotic stroke. The automated version of the tapered beam test may therefore serve as an extension to the toolkit of behavioral neuroscience methods in rodents as a quick yet sensitive evaluation of (unilateral) motor deficits.

Acknowledgements

This work was supported by the Canadian Institute of Health Research Foundation (FDN143209), the Brain Canada Neurophotonics Platform, and the Leducq Foundation. We thank Luis Bolaños and Jessica Lee for assistance with electronic artwork and video analysis and Jamie Boyd for advice with software and electronics.

Appendix A. Supplementary data

Supplementary data associated with this article can be found, in the online version, at http://dx.doi.org/10.1016/j.jneumeth.2017.08.030.

References

Balbi, M., Vanni, M.P., Silasi, G., Sekino, Y., Bolaños, L., LeDue, J.M., Murphy, T.H., 2017. Targeted ischemic stroke induction and mesoscopic imaging assessment of blood flow and ischemic depolarization in awake mice. Neurophotonics 4, 35001, http://dx.doi.org/10.1117/1.NPh.4.3.035001.

Bolaños, F., LeDue, J.M., Murphy, T.H., 2017. Cost effective raspberry pi-based radio frequency identification tagging of mice suitable for automated in vivo imaging. J. Neurosci. Methods 276, 79–83, http://dx.doi.org/10.1016/j.jneumeth.2016.11.011.

Brooks, S.P., Dunnett, S.B., 2009. Tests to assess motor phenotype in mice: a user's guide. Nat. Rev. Neurosci. 10, 519–529, http://dx.doi.org/10.1038/nrn2652.

Bye, N., Habgood, M.D., Callaway, J.K., Malakooti, N., Potter, A., Kossmann, T., Morganti-Kossmann, M.C., 2007. Transient neuroprotection by minocycline following traumatic brain injury is associated with attenuated microglial activation but no changes in cell apoptosis or neutrophil infiltration. Exp. Neurol. 204, 220–233, http://dx.doi.org/10.1016/j.expneurol.2006.10.013.

Caleo, M., 2015. Rehabilitation and plasticity following stroke: insights from rodent models. Neuroscience 311, 180–194, http://dx.doi.org/10.1016/j.neuroscience.2015.10.029.

Chen, C.-C., Gilmore, A., Zuo, Y., 2014. Study motor skill learning by single-pellet reaching tasks in mice. J. Vis. Exp., 1–7, http://dx.doi.org/10.3791/51238.

Corrigan, F., Vink, R., Blumbergs, P.C., Masters, C.L., Cappai, R., van den Heuvel, C., 2012. Evaluation of the effects of treatment with sAPPα on functional and histological outcome following controlled cortical impact injury in mice. Neurosci. Lett. 515, 50–54, http://dx.doi.org/10.1016/j.neulet.2012.03.017.

Farr, T.D., Whishaw, I.Q., 2002. Quantitative and qualitative impairments in skilled reaching in the mouse (Mus musculus) after a focal motor cortex stroke. Stroke 33, 1869–1875, http://dx.doi.org/10.1161/01.STR.0000020714.48349.4E.
Fenrich, K.K., May, Z., Hurd, C., Boychuk, C.E., Kowalczewski, J., Bennett, D.J., Whishaw, I.Q., Fouad, K., 2015. Improved single pellet grasping using automated ad libitum full-time training robot. Behav. Brain Res. 281, 137–148, http://dx.doi.org/10.1016/j.bbr.2014.11.048.
GraphPad Software, 2017. GraphPad Prism Version 7.
Lipsanen, A., Hiltunen, M., Jolkkonen, J., 2011. Chronic ibuprofen treatment does not affect the secondary pathology in the thalamus or improve behavioral outcome in middle cerebral artery occlusion rats. Pharmacol. Biochem. Behav. 99, 468–474, http://dx.doi.org/10.1016/j.pbb.2011.04.019.
Madisen, L., Mao, T., Koch, H., Zhuo, J., Berenyi, A., Fujisawa, S., Hsu, Y.-W.A., Garcia, A.J., Gu, X., Zanella, S., Kidney, J., Gu, H., Mao, Y., Hooks, B.M., Boyden, E.S., Buzsáki, G., Ramirez, J.M., Jones, A.R., Svoboda, K., Han, X., Turner, E.E., Zeng, H., 2012. A toolbox of Cre-dependent optogenetic transgenic mice for light-induced activation and silencing. Nat. Neurosci. 15, 793–802, http://dx.doi.org/10.1038/nn.3078.
Mar, A.C., Horner, A.E., Nilsson, S.R.O., Alsiö, J., Kent, B.A., Kim, C.H., Holmes, A., Saksida, L.M., Bussey, T.J., 2013. The touchscreen operant platform for assessing executive function in rats and mice. Nat. Protoc. 8, 1985–2005, http://dx.doi.org/10.1038/nprot.2013.123.
Metz, G.A., Whishaw, I.Q., 2009. The ladder rung walking task: a scoring system and its practical application. J. Vis. Exp., 2–5, http://dx.doi.org/10.3791/1204.
Murphy, T.H., Boyd, J.D., Bolaños, F., Vanni, M.P., Silasi, G., Haupt, D., LeDue, J.M., 2016. High-throughput automated home-cage mesoscopic functional imaging of mouse cortex. Nat. Commun. 7, 11611, http://dx.doi.org/10.1038/ncomms11611.
Ng, S.Y., Semple, B.D., Morganti-Kossmann, M.C., Bye, N., 2012. Attenuation of microglial activation with minocycline is not associated with changes in neurogenesis after focal traumatic brain injury in adult mice. J. Neurotrauma 29, 1410–1425, http://dx.doi.org/10.1089/neu.2011.2188.
R Core Team, 2017. R: A Language and Environment for Statistical Computing.
Schaefer, A.T., Claridge-Chang, A., 2012. The surveillance state of behavioral automation. Curr. Opin. Neurobiol. 22, 170–176, http://dx.doi.org/10.1016/j.conb.2011.11.004.
Schallert, T., Tillerson, J.L., 2000. Intervention strategies for degeneration of dopamine neurons in parkinsonism: optimizing behavioral assessment of outcome. In: Emerich, D.F., Dean, R.L., Sanberg, P.R. (Eds.), Central Nervous System Diseases: Innovative Animal Models from Lab to Clinic. Humana, Totowa, New Jersey, pp. 131–151.
Schallert, T., Woodlee, M.T., Fleming, S.M., 2002. Disentangling multiple types of recovery from brain injury recovery of function. Pharmacol. Cereb. Ischemia, 201–216.
Semple, B.D., Bye, N., Ziebell, J.M., Morganti-Kossmann, M.C., 2010. Deficiency of the chemokine receptor CXCR2 attenuates neutrophil infiltration and cortical damage following closed head injury. Neurobiol. Dis. 40, 394–403, http://dx.doi.org/10.1016/j.nbd.2010.06.015.
Silasi, G., Xiao, D., Vanni, M.P., Chen, A.C.N., Murphy, T.H., 2016. Intact skull chronic windows for mesoscopic wide-field imaging in awake mice. J. Neurosci. Methods 267, 141–149, http://dx.doi.org/10.1016/j.jneumeth.2016.04.012.
Sorge, R.E., Martin, L.J., Isbester, K. a., Sotocinal, S.G., Rosen, S., Tuttle, A.H., Wieskopf, J.S., Acland, E.L., Dokova, A., Kadoura, B., Leger, P., Mapplebeck, J.C.S., McPhail, M., Delaney, A., Wigerblad, G., Schumann, A.P., Quinn, T., Frasnelli, J., Svensson, C.I., Sternberg, W.F., Mogil, J.S., 2014. Olfactory exposure to males, including men, causes stress and related analgesia in rodents. Nat. Methods 11, 629–632, http://dx.doi.org/10.1038/nmeth.2935.
Spanevello, M.D., Tajouri, S.I., Mirciov, C., Kurniawan, N., Pearse, M.J., Fabri, L.J., Owczarek, C.M., Hardy, M.P., Bradford, R.A., Ramunno, M.L., Turnley, A.M., Ruitenberg, M.J., Boyd, A.W., Bartlett, P.F., 2013. Acute delivery of EphA4-Fc improves functional recovery after contusive spinal cord injury in rats. J. Neurotrauma 30, 1023–1034, http://dx.doi.org/10.1089/neu.2012.2729.
Tarlac, V., Kelly, L., Nag, N., Allen-Graham, J., Anderson, R.P., Storey, E., 2013. HLA-DR3-DQ2 mice do not develop ataxia in the presence of high titre anti-gliadin antibodies. Cerebellum 12, 370–376, http://dx.doi.org/10.1007/s12311-012-0425-z.
Tennant, K.A., Jones, T.A., 2009. Sensorimotor behavioral effects of endothelin-1 induced small cortical infarcts in C57BL/6 mice. J. Neurosci. Methods 181, 18–26, http://dx.doi.org/10.1016/j.jneumeth.2009.04.009.
van Rossum, G., 1995. Python.
Weissbrod, A., Shapiro, A., Vasserman, G., Edry, L., Dayan, M., Yitzhaky, A., Hertzberg, L., Feinerman, O., Kimchi, T., 2013. Automated long-term tracking and social behavioural phenotyping of animal colonies within a semi-natural environment. Nat. Commun. 4, 1–10, http://dx.doi.org/10.1038/ncomms3018.
Yang, S.H., Gustafson, J., Gangidine, M., Stepien, D., Schuster, R., Pritts, T.A., Goodman, M.D., Remick, D.G., Lentsch, A.B., 2013. A murine model of mild traumatic brain injury exhibiting cognitive and motor deficits. J. Surg. Res. 184, 981–988, http://dx.doi.org/10.1016/j.jss.2013.03.075.
Zhao, C.S., Puurunen, K., Schallert, T., Sivenius, J., Jolkkonen, J., 2005. Effect of cholinergic medication, before and after focal photothrombotic ischemic cortical injury, on histological and functional outcome in aged and young adult rats. Behav. Brain Res. 156, 85–94, http://dx.doi.org/10.1016/j.bbr.2004.05.011.